Crystal Engineering

DOI: 10.1002/ange.201410730

Designing Elastic Organic Crystals: Highly Flexible Polyhalogenated *N*-Benzylideneanilines**

Soumyajit Ghosh, Manish Kumar Mishra, Sourabh B. Kadambi, Upadrasta Ramamurty, and Gautam R. Desiraju**

Abstract: *The intermolecular interactions and structural features in crystals of seven halogenated N-benzylideneanilines (Schiff bases), all of which exhibit remarkable flexibility, were examined to identify the common packing features that are the raison d'être for the observed elasticity. The following two features, in part related, were identified as essential to obtain elastic organic crystals: 1) A multitude of weak and dispersive interactions, including halogen bonds, which may act as structural buffers for deformation through easy rupture and reformation during bending; and 2) corrugated packing patterns that would get interlocked and, in the process, prevent long-range sliding of molecular planes.*

The resistance of a crystalline material to both elastic and plastic deformation depends on the crystal structure as well as the atomic bonding characteristics.[1,2] In the context of metallic materials, these characteristics are fixed for any given metal and the elastic modulus cannot therefore be altered.[3] On the other hand, the resistance of a metal to plastic deformation, that is strength, can be enhanced significantly by decreasing the dislocation mobility; this can be achieved by recourse to alloying and other strategies.[4] Molecular crystals are quite distinctive and offer a much larger canvas for the design of materials with unique combinations of mechanical properties, and also with implications for biological materials.[5] In these solids, crystal engineering principles may be gainfully employed so that both the type and number of intermolecular interactions as also the crystal structure can be varied in a predictable manner.[6] However, this exercise requires a full and comprehensive understanding of the structural factors and features that enhance elastic and plastic responses of organic crystals.[1,2] While the interrelations between the chemical, physical, and functional properties and the underlying crystal structures of molecular materials are well understood by now, efforts to establish such connections with mechanical responses are scarce. This is surprising in view of the fact that mechanical properties play a vital role in the applications of organic crystals, such as in pharmaceutical manufacturing.[7] Most structural materials in nature are also organic compounds. Recognition of all of this has lately led to a spurt in research on mechanical properties of molecular crystals.

Recent studies have established that plastic deformation in organic crystals may be rationalized on the basis of anisotropic packing, that is, the presence of strong and weak interactions in nearly orthogonal directions, and the availability of slip systems (close packed, and hence widely separated, planes).[2] These conditions are, in part, interrelated. However, no such general rules are available when it comes to designing highly flexible, that is elastic, molecular crystals. Ghosh and Reddy, who examined the caffeine-4-chloro-3-nitrobenzoic acid cocrystal, suggested that its elastic nature is due to the isotropic interlocking of interactions: there are weak and dispersive C−H···π interactions in three nearly perpendicular directions.[1a] Mukherjee and Desiraju rationalized the significant elastic bending in 4-bromo-3-chlorophenol on the basis of comparable hydrogen bonding and halogen bonding in different directions.[1b,8] Taken together, these results suggest that plastic deformation in organic crystals is a consequence of structural anisotropy, while elastic deformation seems to arise from isotropic molecular packing. In the present study, we examine the mechanical behavior of a family of seven halogenated *N*-benzylideneanilines (Schiff bases) and identify the common underlying structural features that cause these crystals to be highly flexible. Accordingly, moves can be made toward systematic design strategies.

Acicular crystals, 3 to 5 mm in length and 0.02–0.05 mm in thickness, of the molecular series **EC1** through **EC7** (Scheme 1) were synthesized by slow evaporation of MeOH solutions containing one equivalent each of the corresponding dichlorobenzaldehyde and halogen-substituted aniline. Analysis of the crystal structures of **EC1** through **EC7** (see the Supporting Information) reveals that they are closely related to one another. Polymorphism was not observed in any of these compounds even after exhaustive crystallization experiments. Compounds **EC2** and **EC4** are selected here as

[*] Dr. S. Ghosh,[+] M. K. Mishra,[+] Prof. G. R. Desiraju
Solid State and Structural Chemistry Unit
Indian Institute of Science, Bangalore 560 012 (India)
E-mail: desiraju@sscu.iisc.ernet.in
S. B. Kadambi
Department of Materials Engineering
Indian Institute of Science, Bangalore 560 012 (India)
Prof. U. Ramamurty
Department of Materials Engineering
Indian Institute of Science, Bangalore 560 012 (India)
and
Center of Excellence for Advanced Materials Research
King Abdulaziz University, Jeddah 21589 (Saudi Arabia)
E-mail: ramu@materials.iisc.ernet.in
[+] These authors contributed equally to this work.

[**] S.G. thanks DST for a Young Scientist Fellowship. M.K.M. thanks CSIR, India for a Senior Research Fellowship. U.R. and G.R.D. thank the Department of Science and Technology, India for J. C. Bose Fellowships.

Supporting information for this article is available on the WWW under http://dx.doi.org/10.1002/anie.201410730.

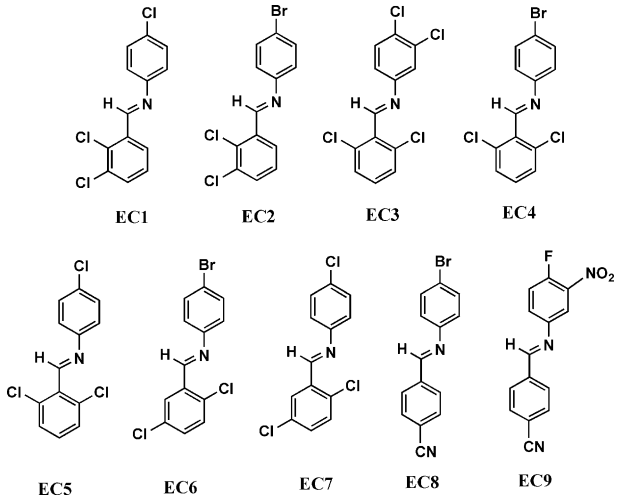

Scheme 1. Molecules **EC1**–**EC7**, which give elastic bendable crystals; in contrast, **EC8** and **EC9** crystallize in brittle forms.

representative examples to highlight relevant structural features. 2,3-Dichlorobenzylidine-4-bromoaniline (**EC2**) crystallizes in the triclinic space group $P\bar{1}$ with one molecule in the asymmetric unit (Figure 1 a). The aromatic rings are in a *trans* conformation around the CH=N bond. The molecules are connected via C–H···N dimers (D, d, θ: 3.72 Å, 2.79 Å, 168.9°) and C–H···Cl (3.76 Å, 3.12 Å, 127°) hydrogen bonds to give zigzag tapes parallel to the crystal long direction, [010] (Figure 1 b). The molecules in the tape are further π···π stacked parallel to the a axis (3.913 Å) to give a corrugated sheet in the (001) plane. Each neighboring tape is connected via C–H···Cl (3.76 Å, 3.02 Å, 135.97°) and C–H···Br (3.78 Å, 3.221 Å, 119.62°) hydrogen bonds and type I Br···Br (3.89 Å, $\theta_1 = \theta_2 = 124.81°$) halogen bond interactions (Figure 1 b) to form corrugated sheets parallel to the (100) plane (Figure 1 a). The packing is isotropic: there is π···π stacking along [100], C–H···Cl along [010], and type I Br···Br and C–H···Br along [001] and these three interaction types are energetically comparable (1–3 kcal mol^{-1} each). The interactions are all of moderate strength and mildly electrostatic to non-polar.

2,6-Dichlorobenzylidine-4-bromoaniline (**EC4**) crystallizes in the orthorhombic space group $Pca2_1$ with one molecule in the asymmetric unit. The packing (Figure 2 a) is similar to that of **EC2**; molecules are joined by C–H···Br hydrogen bonds (4.84 Å, 3.04 Å, 156.13°; 4.44 Å, 3.12 Å, 122.67°) giving zigzag chains parallel to the needle axis a (Figure 2 b). There is a twisting of aromatic rings across the CH=N kink in the molecule as per the *trans*-conformation. Neighboring 1D chains, which are parallel and offset, are further connected via weak type II Cl···Br (3.54 Å, $\theta_1 = 156.93°$, $\theta_2 = 112.73°$; 3.56 Å, $\theta_1 = 101.73°$, $\theta_2 = 167.43°$) halogen bonds and multiple C–H···Cl (3.86 Å, 2.97 Å, 154.25°; 3.73 Å, 3.12 Å, 123.62°) hydrogen bond interactions (Figure 2 b) resulting in 2D corrugated sheets in the (010) plane (Figure 2 a). In the individual chain, molecules form π···π stacks (3.99 Å) parallel to the b axis resulting in 2D corrugated sheets in the (001) plane. Once again there are comparable but moderate interactions along the three major directions.

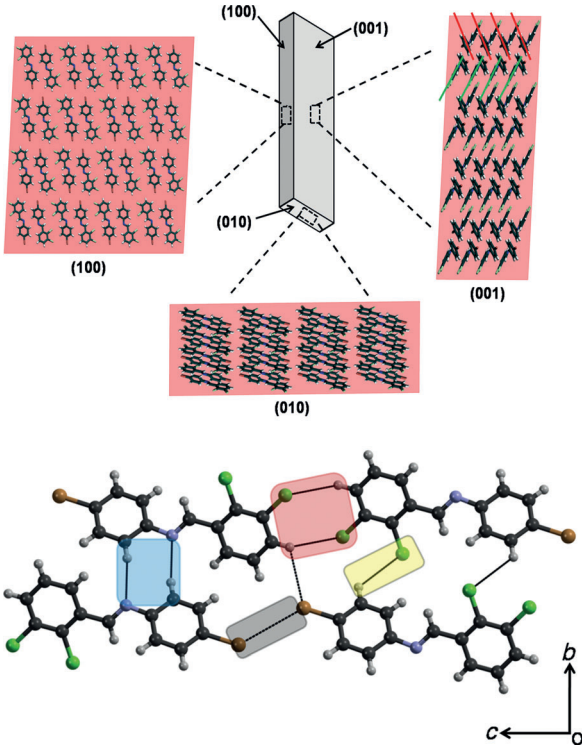

Figure 1. a) Crystal packing in **EC2**. Crystal morphology with face indices. Packing viewed down (001), (100), and (010) faces. Note that when the crystals are bent along [001], the (001) major faces are those that experience maximum tensile or contractile strains. In the major bendable face (001), red and green lines indicate a criss-cross arrangement (51° acute angle), which hinders long range of movement of molecules during bending. b) Hydrogen bond and halogen bond pattern with color code: C–H···N dimer (blue), C–H···Cl (yellow), C–H···Cl dimer (red), type I Br···Br (gray).

As mentioned already, packing patterns for the other crystals (**EC1**, **EC3**, **EC5**, **EC6**, **EC7**) in this family are similar. In **EC1**, which crystallizes in the orthorhombic space group $Pna2_1$, molecules are in a herringbone arrangement parallel to the (001) plane. Molecules in neighboring tapes are further connected via C–H···N (3.59 Å, 2.92 Å, 130.52°) and C–H···Cl (3.72 Å, 3.06 Å, 127.17°; 3.75 Å, 2.90 Å, 143.94°; 3.70 Å, 3.08 Å, 125.05°) interactions to give 2D corrugated sheets in the (001) plane. Moreover, molecules in the tape are π···π stacked parallel to the c axis (3.84 Å) leading to corrugated 2D sheet in the (010) plane. When viewed down the (010) face, it is seen that molecules are in a criss-cross arrangement. Similarly, in **EC3** (space group $P2_1/c$) molecules link in corrugated chains via C–H···Cl hydrogen bonds (3.53 Å, 2.855 Å, 129.15°) and these chains are further connected via two type II; quasi type I/II Cl···Cl (3.43 Å, $\theta_1 = 99.18°$, $\theta_2 = 169.82°$; 3.58 Å, $\theta_1 = 149.56°$, $\theta_2 = 121.42°$) halogen bond interactions parallel to (010). In **EC5** (space group $Pca2_1$) molecules link in corrugated chains via C–H···Cl (3.56 Å, 2.90 Å, 127.61°; 3.67 Å, 2.92 Å, 136.31°) hydrogen bonds interactions parallel to the a axis. The neighboring chains are further connected via two type II Cl···Cl (3.35 Å, $\theta_1 = 103.61°$, $\theta_2 = 164.57°$; 3.32 Å, $\theta_1 = 119.74°$, $\theta_2 = 163.05°$) halogen bond and C–H···N (3.55 Å, 2.63 Å, 161.99°) hydrogen bond interactions to give 2D corrugated sheets parallel to the (010)

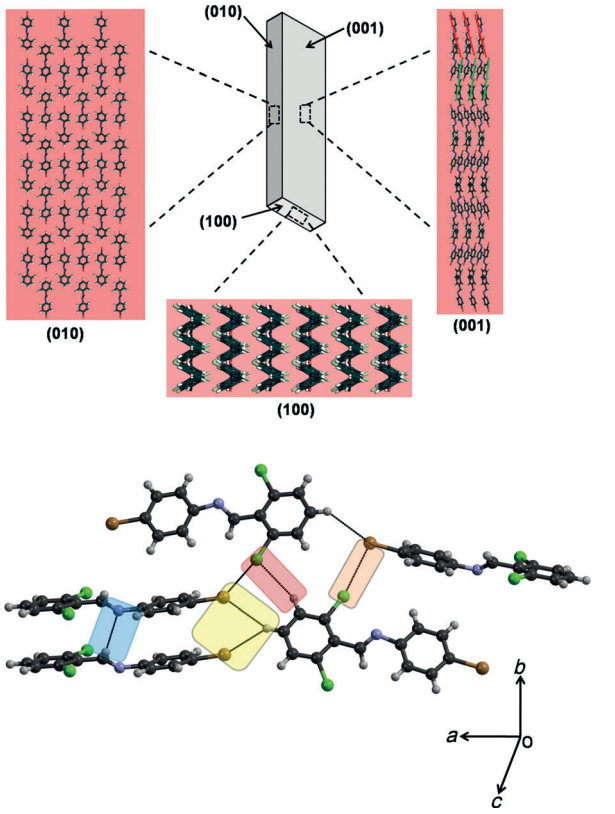

Figure 2. a) Crystal packing in **EC4.** Crystal morphology with face indices. Projections viewed down the major face (001), and smaller (010) and (100) faces. Note that on face (001), red and green lines indicate the criss-cross arrangement of molecular layers, which prevents their easy slippage during deformation. b) Hydrogen bond and halogen bond pattern with color code: C–H···N (blue), C–H···Br (yellow), C–H···Cl (pink), type II Cl···Br (orange).

plane. Criss-cross packing can be viewed down the (001) plane, which is the major face in **EC5** (see the Supporting Information). In **EC6** and **EC7** too, molecules lie in corrugated tapes parallel to the crystal axis *b*. In **EC6**, C–H···Cl (3.68 Å, 2.98 Å, 131.42°) and type I Cl···Br (3.43 Å, $\theta_1 = 170.42°$, $\theta_2 = 160.05°$) interactions are involved giving corrugated tapes whereas in **EC7**, various C–H···Cl (3.60 Å, 2.94 Å, 127.52°; 3.72 Å, 2.92 Å, 143.21°; 3.77 Å, 2.88 Å, 157.70°) hydrogen-bond interactions are involved. In both **EC6** and **EC7**, the tapes are π···π stacked parallel to the *a* axis to give corrugated 2D sheets in the (001) plane. Here too, the criss-cross arrangement is visible on the (001) face. In summary, there are two relevant structural features in these seven structures: comparably weak interactions in three major directions giving rise to packing isotropy and second, a criss-cross packing, which promotes interlocking of structural patterns so as to hinder long range molecular movement.

Individual crystals were extracted and subjected to qualitative mechanical tests to assess their mechanical response. These were conducted by holding each crystal against a pair of forceps and then pushing the crystal at the mid-span with a metallic needle from the opposite side (Figure 3). Results indicate that all crystals in this series can be bent easily without breakage (see videos in the Supporting Information). They regain their original shape when the needle is retracted, indicating that the observed deformation is essentially elastic. The bending process can be repeated many times, implying that the fatigue process does not occur or is minimal. When the crystals are bent beyond a threshold limit, the crystals break into two pieces rather than deform permanently (Figure 3i). In such cases, the broken halves become straight after fracture and are themselves elastically bendable. The maximum elastic strain, estimated using maximum curvature of the bent crystals and the Euler–Bernoulli beam-bending theory,[9] is about 2% (see the Supporting Information for the estimation procedures utilized). It may also be noted that the physical dimensions of the selected crystals **EC1** through **EC7** are all very similar and within the ranges mentioned earlier. Therefore the mechanical responses may be properly correlated with the respective crystal structures, or in other words, they are not the result of trivial aspects such as varying crystal thickness.

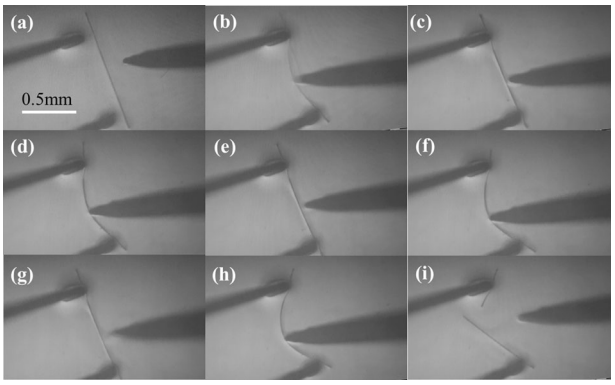

Figure 3. Snapshots (a) through (h) of crystal **EC1** to show bending cycles induced with a pair of forceps and a metallic needle. (i) The crystal breaks when it is bent beyond a threshold limit.

Next, a nanoindenter, the utility of which for measuring the mechanical properties of molecular crystals especially in the context of crystal engineering has been successfully established,[10] was employed to quantitatively ascertain the elastic nature of the crystals. Instead of indenting, the instrument is utilized to conduct tests in the three-point bend[11] configuration wherein a high load cell was used to facilitate greater than 5 μm displacement, and with the accompanying features of high load and displacement resolutions that this cell offers (see the Supporting Information for details).

Representative load–displacement (*P*–*h*) curves obtained on an **EC6** crystal are displayed in Figure 4. The crystal was first subjected to a maximum displacement, h_{max}, of 5 μm before unloading. In the subsequent cycle, h_{max} was increased to 10 μm, that is, by a 5 μm increment, and this process was continued up to $h_{max} = 35$ μm. A higher h_{max} could not be achieved owing to the maximum allowable displacement range of the nanoindenter. The loading segments of the *P*–*h* curves were observed to be nearly linear in all cases and overlap. This is the reason for not displaying all load–unload curves in Figure 4, as clarity would be lost in doing so. Analyses using simple mechanics (see the Supporting Information) indicate that $h_{max} = 35$ μm corresponds to a flexural

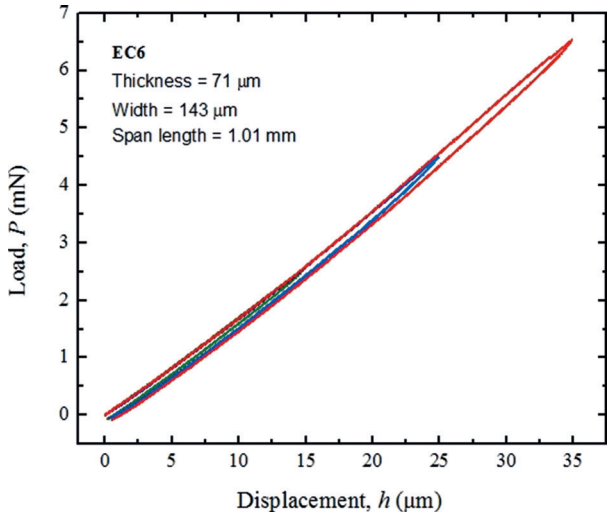

Figure 4. Representative load-displacement (*P*–*h*) curves obtained (**EC6**) using the three-point bend test carried out using a nanoindenter, with increasing maximum displacements at the center of the span length.

strain of about 1%. While slight nonlinearity is observed in the unloading segment of the *P*–*h* curve, it reverts back to zero displacement upon complete unloading, indicating the ability of the crystals for shape recovery. All these observations confirm the elastic nature of the series of molecular crystals examined in this study.

Before discussing the structural origins for the observed elasticity, it is pertinent to contrast the obtained elastic strain (2%) with those seen in commonly used crystalline materials. In most crystalline alloys the maximum elastic strain (or yield strain) is only about 0.5%, beyond which they undergo permanent deformation.[12a] While higher yield strains have been reported for free standing nanowires, amorphous alloys and in some polymers and biomaterials,[12] the elastic response observed in the **EC1** to **EC7** series of organic crystals can be considered remarkably high, which is due to the following two important and complementary features that are common to all of them.

The first is weak, dispersive, and numerous C–H···Cl, C–H···Br, and halogen bond (Cl···Cl, Cl···Br, Br···Br) interactions along the crystallographic planes that get stretched during bending. These interactions, which can be readily broken or reformed, ensure free molecular motion during bending; they allow the molecules to move over one another in the outer and inner arcs. Thus, the weak interactions provide "structural buffering" during deformation. The halogen bonds in these crystals, which use large atoms at the molecular peripheries, are especially relevant in this regard and their restorative ability is expected to be important. A notable aspect is that halogen bonds are directional enough to favor certain specific structural patterns, yet they are directionless enough that they act as restoring forces upon deformation. Their nature, which is intermediate between hydrogen bonds and van der Waals interactions, is somewhat critical for their structural role in these systems. The importance of halogen bonds in maintaining crystal elasticity can be further illustrated through a comparison of **EC2** and **EC6**. Both crystals are highly elastic but **EC6** is stiffer (bending stiffness of **EC2** and **EC6** are 91 and 179 $N\,m^{-1}$ respectively). The crystal packing is very similar save for the fact that the weaker Br···Br interaction (3.89 Å) in **EC2** is replaced by a stronger Br···Cl interaction (3.43 Å) in **EC6** accounting for its much stiffer nature.

In the second, the crystal packing, while being isotropic in nature, contains features that promote interlocking of crystallographic planes so as to hinder long range molecular movement, which would otherwise lead to plastic (or permanent) deformation during flexing. This can be illustrated with the aid of Figure 1a, wherein (001) planes of **EC2** are those that get stretched during bending. While rupture of the weak C–H···Cl dimer interactions allow for easy sliding here, the acute angle (ca. 50°) between the 1D tapes in neighboring corrugated 2D sheets hinders plastic deformation. In the case of **EC4** (Figure 2a), likewise, the acute angle (ca. 60°) between the two zigzag chains of adjacent corrugated sheets prevents long range molecular movement of molecules during bending. These insulating interactions buffer the molecular movements in a way that is similar to the role of solvent in the caffeine co-crystal solvate, studied earlier by Ghosh and Reddy.[1a] There, the solvent molecules were proposed to act as rollers between comb-like 2D sheets.

To further illustrate that the above mentioned packing features are indeed needed to observe elasticity, we selected two additional systems, **EC8** and **EC9** (Scheme 1), which specifically do not contain these two features. Both these crystals lack the isotropic packing that is required in elastically bendable crystals (see the Supporting Information for details). Also **EC8** has a slip plane that would allow for possible slip upon application of stress, leading to plastic deformation. Other requisite criteria for high elasticity such as halogen bonds or π···π stacking, which might act as a structural buffers during bending are absent in both **EC8** and **EC9** structures. When stress was applied on them, the crystals broke into pieces showing their brittle nature.

In summary, we have identified, on the basis of experiments on a series of *N*-benzylideneanilines, the structural features (schematically illustrated in Figure 5) that are essential to obtain highly flexible organic crystals: 1) Isotropic

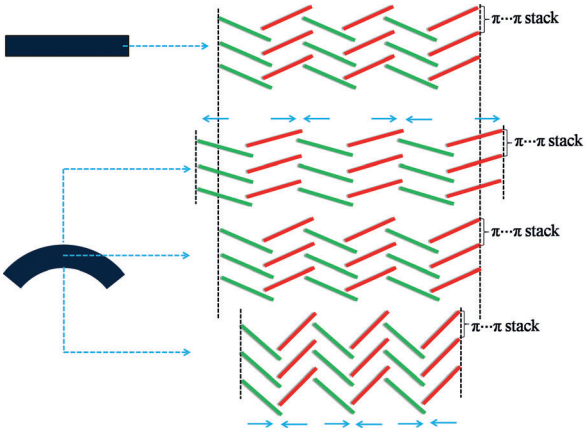

Figure 5. Representation of structural features that give flexibility to molecular crystals.

and uniform distribution of weaker interactions in three orthogonal directions, leading to the formation of pairs of elastic bendable side faces. The weak interactions between molecules, but within tapes or chains, facilitate large elastic strain accommodation during deformation. 2) Interlocked, that is a criss-cross arrangement of molecules either in the same tape or between neighboring tapes in adjacent 2D sheets. This effectively means an absence of slip planes which would have facilitated easy shearing of the molecular layers past each other resulting in plastic deformation. An interlocked arrangement allows for the appearance of hinge joints that restricts long range molecular movement away from the equilibrium positions.

Received: November 4, 2014
Published online: January 13, 2015

Keywords: crystal engineering · elasticity · halogen bonds · mechanical properties · nanoindentation

[1] a) S. Ghosh, C. M. Reddy, *Angew. Chem. Int. Ed.* **2012**, *51*, 10319 – 10323; *Angew. Chem.* **2012**, *124*, 10465 – 10469; b) A. Mukherjee, G. R. Desiraju, *IUCrJ* **2014**, *1*, 49 – 60; c) S. Takamizawa, Y. Miyamoto, *Angew. Chem. Int. Ed.* **2014**, *53*, 6970 – 6973; *Angew. Chem.* **2014**, *126*, 7090 – 7093.

[2] a) C. M. Reddy, M. T. Kirchner, R. C. Gundakaram, G. R. Desiraju, *Chem. Eur. J.* **2006**, *12*, 2222 – 2234; b) C. M. Reddy, G. R. Krishna, S. Ghosh, *CrystEngComm* **2010**, *12*, 2296 – 2314; c) C. M. Reddy, R. C. Gundakaram, S. Basavoju, M. T. Kirchner, K. A. Padmanabhan, G. R. Desiraju, *Chem. Commun.* **2005**, 3945 – 3947; d) C. M. Reddy, K. A. Padmanabhan, G. R. Desiraju, *Cryst. Growth Des.* **2006**, *6*, 2720 – 2731; e) N. K. Nath, L. Pejov, S. M. Nichols, C. Hu, N. Saleh, B. Kahr, P. Naumov, *J. Am. Chem. Soc.* **2014**, *136*, 2757 – 2766; f) M. K. Panda, S. Ghosh, N. Yasuda, T. Moriwaki, G. D. Mukherjee, C. M. Reddy, P. Naumov, *Nat. Chem.* **2014**, DOI: 10.1038/NCHEM.2123.

[3] G. E. Dieter, *Mechanical metallurgy*, McGraw-Hill Book Company, London, **1988**.

[4] D. Tabor, *The hardness of metals*, Oxford University Press, Oxford, **1951**.

[5] a) P. Fratzl, F. G. Barth, *Nature* **2009**, *462*, 442 – 448; b) M. A. Garcia-Garibay, *Angew. Chem. Int. Ed.* **2007**, *46*, 8945 – 8947; *Angew. Chem.* **2007**, *119*, 9103 – 9105; c) S. Lv, D. M. Dudek, Y. Cao, M. M. Balamurali, J. Gosline, H. Li, *Nature* **2010**, *465*, 69 – 73; d) Y. Cao, H. Li, *Nat. Mater.* **2008**, *3*, 512 – 516; e) S. Keten, Z. Xu, B. Ihle, M. J. Buehler, *Nat. Mater.* **2010**, *9*, 359 – 367; f) F. Vollrath, D. Porter, *Soft Matter* **2006**, *2*, 377 – 385; g) P. E. Marszalek, *Nature* **1999**, *402*, 100 – 103; h) P. E. Marszalek, A. F. Oberhauser, Y. P. Pang, J. M. Fernandez, *Nature* **1998**, *396*, 661 – 664; i) M. S. Kellermayer, S. B. Smith, H. L. Granzier, C. Bustamante, *Science* **1997**, *276*, 1112 – 1116.

[6] a) G. R. Desiraju, *Crystal Engineering: The Design of Organic Solids*, Elsevier, New York, **1989**; b) G. R. Desiraju, *Angew. Chem. Int. Ed.* **2007**, *46*, 8342 – 8356; *Angew. Chem.* **2007**, *119*, 8492 – 8508; c) E. R. T. Tiekink, J. J. Vittal, *Frontiers in Crystal Engineering*, Wiley, Chichester, UK, **2006**; d) G. R. Desiraju, *J. Am. Chem. Soc.* **2013**, *135*, 9952 – 9967.

[7] a) S. Varughese, M. S. R. N. Kiran, K. A. Solanko, A. D. Bond, U. Ramamurty, G. R. Desiraju, *Chem. Sci.* **2011**, *2*, 2236 – 2242; b) S. Karki, T. Friščić, L. Fábián, P. R. Laity, G. M. Day, W. Jones, *Adv. Mater.* **2009**, *21*, 3905 – 3909; c) F. P. A. Fabbiani, D. R. Allan, W. I. F. David, A. J. Davidson, A. R. Lennie, S. Parsons, C. R. Pulham, J. E. Warren, *Cryst. Growth Des.* **2007**, *7*, 1115 – 1124; d) M. K. Mishra, P. Sanphui, U. Ramamurty, G. R. Desiraju, *Cryst. Growth Des.* **2014**, *14*, 3054 – 3061.

[8] a) P. Metrangolo, H. Neukirch, T. Pilati, G. Resnati, *Acc. Chem. Res.* **2005**, *38*, 386 – 395; b) A. Priimagi, G. Cavallo, P. Metrangolo, G. Resnati, *Acc. Chem. Res.* **2013**, *46*, 2686 – 2695; c) A. Mukherjee, S. Tothadi, G. R. Desiraju, *Acc. Chem. Res.* **2014**, *47*, 2514 – 2524.

[9] S. Timoshenko, *History of strength of materials*, McGraw-Hill, New York, **1953**.

[10] a) G. Kaupp, M. R. Naimi-Jamal, *CrystEngComm* **2005**, *7*, 402 – 410; b) G. Kaupp, J. Schmeyers, U. D. Hangen, *J. Phys. Org. Chem.* **2002**, *15*, 307 – 313; c) S. Ghosh, A. Mondal, M. S. R. N. Kiran, U. Ramamurty, C. M. Reddy, *Cryst. Growth Des.* **2013**, *13*, 4435 – 4441; d) S. Varughese, M. S. R. N. Kiran, U. Ramamurty, G. R. Desiraju, *Angew. Chem. Int. Ed.* **2013**, *52*, 2701 – 2712; *Angew. Chem.* **2013**, *125*, 2765 – 2777; e) U. Ramamurty, J. Jang, *CrystEngComm* **2014**, *16*, 12 – 23; f) M. K. Mishra, S. Varughese, U. Ramamurty, G. R. Desiraju, *J. Am. Chem. Soc.* **2013**, *135*, 8121 – 8124; g) M. K. Mishra, G. R. Desiraju, U. Ramamurty, A. D. Bond, *Angew. Chem. Int. Ed.* **2014**, *53*, 13102 – 13105; *Angew. Chem.* **2014**, *126*, 13318 – 13321; h) E. C. Spencer, M. S. R. N. Kiran, W. Li, U. Ramamurty, N. L. Ross, A. K. Cheetham, *Angew. Chem. Int. Ed.* **2014**, *53*, 5583 – 5586; *Angew. Chem.* **2014**, *126*, 5689 – 5692; i) L. Zhu, F. Tong, C. Salinas, M. K. Al-Muhanna, F. S. Tham, D. Kisailus, R. O. Al-Kaysi, C. J. Bardeen, *Chem. Mater.* **2014**, *26*, 6007 – 6015.

[11] S. Timoshenko, *Strength of materials*, D. Van Nostrand Company, New York, **1940**.

[12] a) M. Telford, *Mater. Today* **2004**, *7*, 36 – 43; b) E. W. Wong, *Science* **1997**, *277*, 1971 – 1975; c) J. Park, R. S. Lakes, *Biomaterials: An Introduction*, 3rd ed., Springer, New York, **2007**; d) K. Otsuka, X. Ren, *Prog. Mater. Sci.* **2005**, *50*, 511 – 678.

